Numerical Study of the Critical Layer in a Rotating Fluid

Raymond Sedney* and Nathan Gerber†
U.S. Army Ballistic Research Laboratory, Aberdeen Proving Ground, Maryland

The unsteady motion of a fluid that fills a spinning cylinder is considered. Nonaxisymmetric, viscous perturbations on the spin-up basic flow are used to study the wave motion. The numerical solution of the spin-up eigenvalue problem is discussed. A critical layer always exists for small time but evanesces at a time depending on specific parameters. Time histories of eigenvalues and critical levels are presented, along with typical effects of the critical layer on eigenfunctions and phase of the velocity. Comparison with experiment is shown.

Introduction

THE unsteady motion of a fluid that fills a spinning right-circular cylinder is considered herein. The spin is imparted impulsively to the cylinder, and the spin-up of the fluid is perturbed to study the wave motion in the rotating fluid. This is called the spin-up eigenvalue or e.v. problem. Because of boundary layers and the critical layer that exist in the flow, the problem is formulated with viscous perturbations. The physical significance of the critical layer is discussed, as well as how it affects the solution of the numerical problem. For the rotating fluid, the condition for a critical layer is that the wave frequency be an integral multiple of the local angular frequency of the basic circumferential flow.

The application of this work is to the study of the flight of liquid-filled projectiles. These have a proclivity for unusual flight behavior and often are unstable even though the same projectile with a solid payload is stable. A knowledge of the wave motion in the rotating fluid is fundamental to an understanding of the effect of the liquid on the projectile motion.

The frequencies and decay rates of the waves are determined by the complex eigenvalues of the system of perturbation equations. For large time, the fluid approaches solid body rotation; for this state, there is no critical layer and the eigenvalue problem is considerably simpler. The critical layer always exists for small time; it ceases to exist at a time that depends on the parameters of the basic flow and the wave motion.

The physics of the basic flow, spin-up from rest, was presented by Wedemeyer.[1] The flow is determined by Reynolds number $Re = \Omega a^2/\nu$ and aspect ratio $A = c/a$, where Ω is the spin (rad/s), a and c are the radius and half-height of the cylinder, and ν is the kinematic viscosity of the fluid. The model determines the core flow, not that in the endwall boundary layers. The flow can also be determined in a more complete way by solving the Navier-Stokes equations by finite difference methods. For the e.v. problem, it would be impractical to use the finite difference solution for the basic flow.

A discussion of previous attempts to solve the e.v. problem, together with more details of the work presented here, is given in Ref. 2. Experimental data such as velocity fields, pressures, or gyroscopic motion of the container exist for the range of parameters $1 < Re < 10^7$ and $1 \leq A \leq 5$. The spin-up basic flow and the e.v. analyses are restricted to the higher Re by virtue of some asymptotic approximations. The lower bound on Re for applicability of the e.v. results is not generally known. For axisymmetric perturbations it appears to be $\mathcal{O}(10^2)$.[3] At present, the analysis of the rotating fluid problem, per se, is also limited because the boundary layers on the cylinder endwalls, i.e., the Ekman layers, and the Stewartson layer on the sidewall are not included. For application to the projectile problem, the angular motion must be restricted to small angles because the theory is linearized.

Whether or not the effects of the time-dependent spin-up basic flow are important in a projectile flight can be estimated by comparing the characteristic time for spin-up, $\bar{t}_s$, with the time of flight of the projectile. If the former is small compared to the latter, spin-up effects can be neglected. For laminar Ekman layers,

$$\bar{t}_s = (2c/a)\, Re^{\frac{1}{2}}/\Omega = 2/E^{\frac{1}{2}}\Omega \qquad \text{(s)}$$

where $E = \nu/\Omega c^2$ is the Ekman number, which is often used in rotating fluid problems rather than Re. This estimate is derivable from linear spin-up theory[4,5] or the Wedemeyer model. We use the nondimensional characteristic spin-up time $t_s = \Omega \bar{t}_s$. For $Re > 10^5$, approximately, the Ekman layers may be turbulent, in which case the characteristic spin-up time can be estimated by

$$\bar{t}_{st} = (28.6\, c/a)\, Re^{\frac{1}{5}}/\Omega = t_{st}/\Omega \qquad \text{(s)}$$

which can be obtained from the Wedemeyer solution without diffusion for turbulent Ekman layers.[1] These times are not measures of how close the flow is to solid body rotation. A rule of thumb often used, but not always accurate, is that solid body rotation is reached at about $4\bar{t}_s$ after an impulsive angular velocity is applied to the cylinder.

To appreciate these time scales for projectile applications, consider the two cases in Table 1, which presents illustrative numerical results. The parameters in Table 1 are appropriate to a test of small caliber projectiles in a ballistic range for case 1, and to test an artillery projectile for case 2. At the spin-up times the projectiles would be 48 m and 1230 m from the gun for cases 1 and 2, respectively; in both cases, observations on projectile motion could be made at these distances. Partial validation of the theory has been provided by experiments[6] and numerical simulations.[3]

Table 1 Illustrative numerical results[a]

Case	Re	c/a	Ω, rad/s	t_s	$\bar{t}_s$, s
1	4974	3.30	8937	465	0.052
2[b]	1.99×10^6	5.20	754	2646	3.510

[a] Courtesy of Dr. W.P. D'Amico.
[b] Turbulent Ekman layers.

Presented as Paper 84-0342 at the AIAA 22nd Aerospace Sciences Meeting, Reno, Nev., Jan. 9-12, 1984; received March 15, 1984; revision received Aug. 20, 1984. This paper is declared a work of the U.S. Government and therefore is in the public domain.

*Research Scientist, Launch and Flight Division. Member AIAA.
†Aerospace Engineer, Launch and Flight Division. Member AIAA.

The Spin-up Basic Flow

Consider the axisymmetric, time-dependent motion of a fluid that fills a cylinder which, initially at rest, is impulsively brought to a constant angular velocity Ω about its axis. Experimentally, an impulsive start is impossible; the conditions for approximating it and the degree of approximation in some experimental apparatus and in a gun tube are discussed in Ref. 7. A summary of Wedemeyer's results needed herein will be given later.

It is known that the Ekman layers form and become essentially steady in time $2\pi\Omega^{-1}$. Although Wedemeyer[1] showed the crucial importance of the Ekman layers to the spin-up process, his model did not require a solution for the flow in these layers; exclusion of this solution has important consequences for the e.v. problem. Wedemeyer did not point out that a boundary layer on the sidewall, a Stewartson layer, is also required in his model. The flow, excluding that in the wall boundary layers, is called the core flow.

In the following, lengths, velocities, pressure, and time are made nondimensional by a, $a\Omega$, $\rho\Omega^2a^2$, and Ω^{-1}, respectively, where ρ is the liquid density. In the inertial frame, cylindrical coordinates r, θ, z are used, with the origin of z at the center of the cylinder, and the velocities are U, V, W, respectively. Dimensionless time is t. Derivatives are indicated by subscripts.

Wedemeyer's order of magnitude arguments reduce the Navier-Stokes equations for the core flow to

$$V_t + U(V_r + V/r) = Re^{-1}[V_{rr} + (V/r)_r] \qquad (1)$$

and

$$U_z = V_z = P_z = 0 \qquad (2)$$

For $Re \to \infty$ he proposed neglecting the diffusion terms in Eq. (1), so that

$$V_{wt} + U_w(V_{wr} + V_w/r) = 0 \qquad (3)$$

where the subscript w indicates this approximation. Wedemeyer used Eq. (3) rather than Eq. (1) when he applied his model.

To solve Eq. (1) or Eq. (3) a relationship between U and V is necessary. A phenomenological approach was used. Some confusion has appeared in later literature because this step was misinterpreted; the matter is discussed in Ref. 7. The result is

$$U = -k_l(r - V) \qquad k_l = \kappa(a/c)\,Re^{-\frac{1}{2}} = 2\kappa/t_s \qquad (4)$$

for laminar Ekman layers. Wedemeyer proposed $\kappa = 0.443$, but Greenspan[4] suggested $\kappa = 0.5$; the latter often gives results in better agreement with numerical solutions to the Navier-Stokes equations. Other relationships have been proposed.[7] For turbulent Ekman layers

$$U = -k_t(r - V)^{\frac{8}{5}} \qquad k_t = 0.035(a/c)\,Re^{-\frac{1}{5}} = 1/t_{st} \qquad (5)$$

The core flow is assumed to be laminar so that turbulent stresses are not introduced in the right-hand side of Eq. (1).

Using Eq. (4), Eq. (3) can be solved explicitly:

$$V_w = (re^{2k_lt} - 1/r)/(e^{2k_lt} - 1) \qquad \text{for } r > e^{-k_lt} \qquad (6)$$

and $V_w = 0$ otherwise. Therefore, $r = r_f = e^{-k_lt}$ separates rotating and nonrotating fluid where there is a discontinuity in shear; this will be smoothed out by inclusion of diffusion terms, as in Eq. (1). From the continuity equation $W = -(z/r)(rU)_r$. At $r = 1$, $W \neq 0$; thus the Stewartson layer should be included at $r = 1$, but this has yet to be done. Also $W \neq 0$ at the endwalls $z = \pm c/a$.

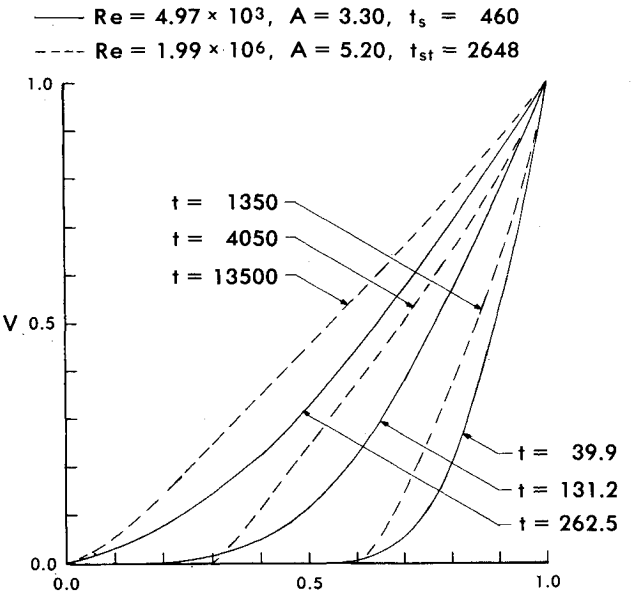

Fig. 1 V vs r for cases 1 and 2 at three times; $\kappa = 0.5$.

The solution to Eq. (1) is required to obtain the e.v. This nonlinear second-order equation is integrated by finite difference methods using some standard techniques for diffusion equations. The boundary conditions are $V(0,t) = 0$, $V(1,t) = 1$ for $t > 0$ and $V(r,0) = 0$ for $0 \le r < 1$. For an impulsive start, a discontinuity in boundary data exists at $r = 1, t = 0$ which was resolved by a local analytic solution.[8] Some examples of the solution to Eq. (1) are shown in Fig. 1 using the parameters of case 1 with Eq. (4) for a laminar Ekman layer, and the parameters of case 2, with Eq. (5) for a turbulent Ekman layer. For each case $V(r,t)$ vs r is shown for three values of t. As $t \to +0$, V tends to the asymptotic solution derived in Ref. 8.

Perturbed Flow

The first step in obtaining the perturbation equations is a standard one and will only be outlined. The velocity components and pressure are expressed as the sum of the spin-up basic flow and the perturbation, e.g., $U^*(r,x,t) + u'(r,\theta,z,t)$. The basic flow is a solution to the Navier-Stokes equations for axisymmetric flow and is designated by an asterisk. The coefficients in the linear perturbation equations are the basic flow variables and their derivatives. These are now approximated by the results from the Wedemeyer model for the core flow. All coefficients containing U^* and W^* and their derivatives with respect to r and z are $\mathcal{O}(1/t_s)$, except for one term discussed below; all those containing V^* are $\mathcal{O}(1)$. Thus, the perturbation equations contain only V, not U and W; they are

$$u'_t + \frac{V}{r}u'_\theta - \frac{2Vv'}{r} = -p'_r + Re^{-1}\left(\nabla^2 u' - \frac{u'}{r^2} - \frac{2v'_\theta}{r^2}\right)$$

$$v'_t + \left(V_r + \frac{V}{r}\right)u' + \frac{V}{r}v'_\theta = -\frac{p'_\theta}{r} + Re^{-1}\left(\nabla^2 v' - \frac{v'}{r^2} + \frac{2u'_\theta}{r^2}\right)$$

$$w'_t + \frac{V}{r}w'_\theta = -p'_z + Re^{-1}\nabla^2 w'$$

$$(ru')_r + v'_\theta + rw'_z = 0 \qquad (7)$$

where ∇^2 is the Laplacian.

These equations govern viscous perturbations of the core flow. If a formal, rational expansion in powers of $Re^{-\frac{1}{2}}$ had been used the viscous or Re^{-1} terms would not have appeared. The inviscid perturbations are adequate, except in the perturbation boundary layer and the critical layer. The viscous

terms could be included by local analyses in these two regions. We have included them in a global sense by retaining the Re^{-1} terms. In the derivation of Eq. (7), one term in the z-momentum equation contains W_r^*. If this is approximated by W_r, that term is not small near $r=1$ because the Wedemeyer model requires a Stewartson layer there, as discussed earlier. Therefore, strictly, Eqs. (7) are valid outside the Stewartson layer; this restriction does not appear to be a serious one. Finally, the time scale for the perturbations is $\mathcal{O}(1)$; whereas, V varies on a time scale $\mathcal{O}(t_s)$ where $t_s \gg 1$ (except for $t \to +0$). This is the basis for the quasisteady assumption wherein t is regarded as a parameter in $V(r,t)$.

Eigenvalue Problem

Mathematical Model

It is convenient to introduce the new coordinate $z' = z + A$. It is assumed that the perturbation can be represented as a superposition of modes. With the quasisteady assumption such a separation of variables is possible. In complex notation

$$u' = \text{Real}\{u(r)\cos Kz' \exp[i(Ct - m\theta)]\} \tag{8}$$

with similar expressions for v' and p'; w' has the same form except for a $\sin Kz'$ factor. Here $K = k\pi/2A$ with $k = 1,2,\ldots$ and $m = 0, \pm 1, \ldots,$ the axial and azimuthal-wave numbers, respectively. The nondimensional complex constant $C = C_R + iC_I$ is the eigenvalue and u, v, w, p are the complex eigenfunctions for the system of differential equations obtained from (7). The dimensional wave frequency is $C_R\Omega$ and the decay rate is $C_I\Omega$.

For the free oscillation problem, the boundary conditions at the endwalls $z' = 0, 2A$ are $u' = v' = w' = 0$ if the complete flow is being perturbed. The modal forms give $w' = 0$ but u' and v' do not satisfy the no-slip condition. Appropriate inner expansions in the Ekman layers are required to correct this. Here the modal form is used without endwall correction, which could have a significant effect on C_I.

From (7) a sixth-order system is obtained:

$$\left[Re^{-1}\left(\Delta_1 - r^{-2}\right) - iM\right] u + \frac{2}{r}\left(V + imr^{-1}Re^{-1}\right) v - p_r = 0$$

$$\left[Re^{-1}\left(\Delta_1 - r^{-2}\right) - iM\right] v - \left(\frac{\partial V}{\partial r} + \frac{V}{r} + \frac{2imRe^{-1}}{r^2}\right) u + \frac{imp}{r} = 0$$

$$\left[Re^{-1}\Delta_1 - iM\right] w + Kp = 0$$

$$(ru)_r - imv + Krw = 0 \tag{9}$$

where

$$\Delta_1 f \equiv f_{rr} + f_r/r - \left[\left(m^2/r^2\right) + K^2\right] f$$

and

$$M(r) = C - mV/r \tag{10}$$

The no-slip boundary conditions at the sidewall require

$$u = v = w = 0 \qquad \text{at } r = 1 \tag{11}$$

The boundary conditions at $r=0$ depend on m (see Ref. 2). For $m = 1$

$$u - iv = w = p = 0 \qquad \text{at } r = 0 \tag{12}$$

The system in Eqs. (9), (11), and (12) is not self-adjoint. Although there is no proof, we assume that the e.v. form is a denumerable, discrete spectrum. With index n used to order the spectrum, the e.v. are C_n. The system must be solved for C_n and the eigenfunctions u_n, v_n, w_n, p_n given V, c/a, Re, m, and k; t enters only through V. If the system were self-adjoint the index n would be the radial mode number. For this non-self-adjoint system it is unclear how to define a mode in a general and unambiguous manner. A mode can be identified for large t by calculating the e.v. for $t \to \infty$, where the radial mode number is known for the solid rotation solution, and then tracked as t decreases. This identification is unambiguous if the critical layer does not exist.

Numerical Method

For $V(r;t)$ obtained from the finite difference solution to Eq. (1), the system (9), (11), and (12) must be integrated for $0 \le r \le 1$; a shooting method with iteration is used. Since Eqs. (9) have a singularity at $r=0$, power series expansions were employed to obtain three solutions near $r=0$ that satisfy Eq. (12) (for $m=1$). Evaluating these at $r=\epsilon$ gives initial conditions for the integration of Eq. (9) over $\epsilon \le r \le 1$. Typically, $\epsilon = 0.001$.[2] Because the coefficient of the highest order derivative, Re^{-1}, is small for Re values of interest, orthonormalization was applied; a modification of Davey's technique[9] was used (see Ref. 10 for details). Typically, it was applied at 50 equally spaced points with an integration interval of 0.001. For large Re, the solution has boundary-layer character near $r=1$, the sidewall perturbation boundary layer, which imposes another constraint on the integration interval.

A value of C must be specified, i.e., the first guess for C_n. Satisfaction of Eq. (11) requires that the characteristic determinant $Z(C) = 0$. If $Z \neq 0$ within a certain tolerance, a new value of C is generated using Newton's method. Muller's method has also been used. Equation (9) is integrated again with the new value of C, etc.

Usually a spin-up e.v. history is required. The computation is started at large t where the first guess can be obtained from the C_n for solid body rotation or its inviscid approximation. For smaller t, the first guess is obtained by extrapolation. As t decreases, this first guess may not be sufficiently close to the desired e.v., and the iteration process will either converge to some other e.v. or, occasionally, diverge. In our computations of C_n this has occurred for $n=2$ at small t. A more detailed searching process is then required. The indicator for this is the shape of the surfaces $Z(C)$, as illustrated by the following example.

For case 1, sections of the surfaces $Z(C)$ will be shown for C in the neighborhood of C_2, at $t=155$. For illustrative purposes it is convenient to plot the single surface $|Z|(C_R, C_I)$, but only sections of that surface with planes C_I = constant are shown in Fig. 2. For the parameters of case 1, $m=1$, $k=3$ and $t=155$, $C_{R2} = 0.072614$ and $C_{I2} = 0.034266$. The shape of the surface changes rapidly in the neighborhood of that point for small changes in C_R and C_I. The first guess must be in an interval $\Delta C_R = 0.0005$ and $\Delta C_I = 0.0003$ about the e.v., that is within about 1% of C_2; otherwise, the iteration converges to C_1. The high peak near the zero of $|Z|$ is symptomatic of this behavior. A method for alleviating this problem was developed. Note that for $n=1$, the $|Z|$ vs C_R curves are monotonic on either side of the e.v., and the first guess can be chosen in a much larger interval; in fact, extrapolation is sufficient.

The time to calculate one C depends on many parameters. For straightforward cases, typical CPU times for one C calculation are 1 min on the CDC 7600 and 5 min on the VAX.

Critical Layer

The Orr-Sommerfeld (O-S) equation that governs the perturbations on a two-dimensional shear flow can be regarded as a prototype for Eq. (9), insofar as stiffness and the existence of critical layers are concerned. A recent review of various aspects of the critical layer in O-S case was given by Stewartson.[11] A

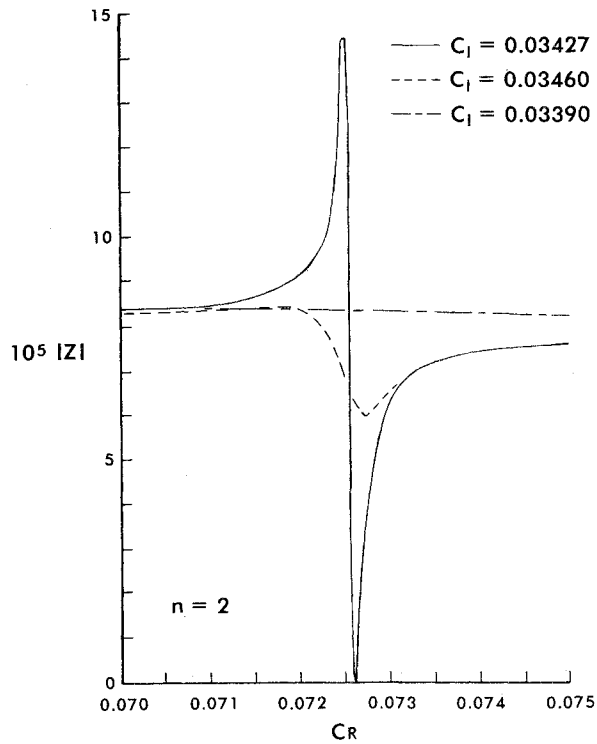

Fig. 2 Magnitude of the characteristic determinant $|Z|$ vs C_R for three values of C_I for case 1; $m = 1, k = 3, t = 155$; $C_{R2} = 0.072614$, $C_{I2} = 0.034266$.

discussion of it using the classical solutions to the O-S equation can be found in Ref. 12. The definition of the critical layer is best appreciated by considering the inviscid limit of the perturbation equations, obtained by setting $Re^{-1} = 0$ in Eq. (9). The order of the system is reduced from six to two. Consider a neutral disturbance, i.e., $C_I = 0$. The coefficient of the highest order derivative contains $M = C - mV/r$ with C real. If $M = 0$ has a real root, r_c, where $0 < r_c < 1$, there is a singular point at the critical level r_c, and the small disturbance assumption is violated. The neighborhood of r_c is called the critical layer. The physical interpretation of

$$C_R = mV/r \tag{13}$$

at $r = r_c$ is that the wave frequency is an integral multiple of the angular frequency of the basic flow, indicating a resonance. If $m = 0$ or if m and C_R have opposite signs there is no critical layer. The nature of the V vs r curves shown in Fig. 1 shows that an r_c always exists for small t if $m \neq 0$ and $\operatorname{sgn} m = \operatorname{sgn} C_R$ but will not exist for large t. There can be a critical layer for each n.

For viscous perturbations the r for which $M = 0$, in general complex, is a turning point of Eq. (9). However, the neighborhood of real r_c obtained from (13) is still called the critical layer. One practical consequence of the existence of the critical layer is that the eigenfunctions can develop high frequency oscillations of large relative amplitude. These occur, most notably, for small t and large Re. The integration scheme and the number of significant figures in the computation must be capable of resolving these in order to get a solution to the e.v. problem for Eq. (9). For the O-S case, Stewartson[11] showed, analytically, that the interval over which the eigenfunctions are "violently oscillatory" is proportional to C_I for a given basic shear flow. This could not be verified by the results for the rotating fluid case.

Results

Some results for eigenfunctions, e.v., and the critical layer will be shown. It is convenient to designate the three wave numbers by the triplet (k, n, m), corresponding to the wave numbers for the (z, r, θ) directions.

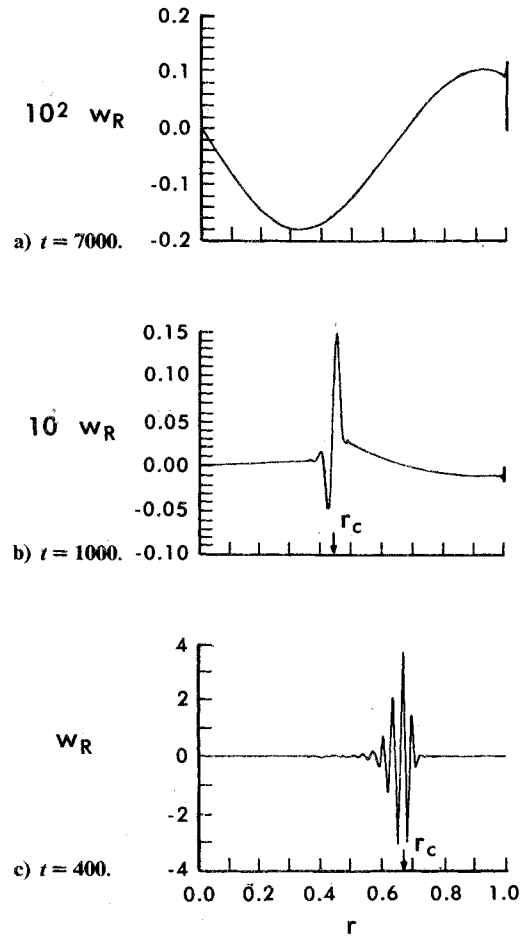

Fig. 3 Eigenfunction Real (w) vs r for $Re = 5 \times 10^5$; $A = 2.679$, mode (5, 1, 1), $t_s = 3788$. Note scale changes.

In Fig. 3 the eigenfunction Real $(w) = w_R$ vs r is shown at three times for $Re = 5 \times 10^5$, $A = 2.679$, $t_s = 3788$ and mode (5,1,1); laminar Ekman layers are assumed. In Fig. 3a, $t = 7000$, $t/t_s = 1.85$, $C_R = 8.354 \times 10^{-2}$, $C_I = 8.363 \times 10^{-4}$, and there is no critical layer. The variation of w_R through the sidewall boundary layer can be barely discerned on this scale. In Fig. 3b, $t = 1000$, $t/t_s = 0.26$, $C_R = 7.060 \times 10^{-2}$, and $r_c = 0.44$ as indicated by the arrow in the figure. The rapid variation of w_R in the neighborhood of r_c is typical of the effects of the critical layer on the eigenfunctions for $Re > 10^4$, approximately. In Fig. 3c, $t = 400$, $t/t_s = 0.11$, $C_R = 3.015 \times 10^{-2}$, $C_I = 8.066 \times 10^{-2}$, and $r_c = 0.66$; outside the critical layer w_R is not zero although it appears to be on this scale. The oscillations of w_R are centered at $r = r_c$. The $\max|w_R|$ is greater in Fig. 3c compared to that of Fig. 3a by a factor of 1900. For the conditions of Fig. 3c, if $\Omega = 628$ rad/s (100 Hz), $\bar{t} = 0.64$ s.

Time histories for C_I and C_2 are shown in Fig. 4 for case 1 and modes (3,1,1) and (3,2,1). The C_{R1} curve has a shallow maximum and minimum for $180 < t < 220$, but on the scale of this figure it appears to be constant. At $t = 45$, it has a maximum which is typical for all C_{R1} vs t curves; note that $C_R = 0$ for $t = 0$. The significance of a maximum in the C_{R1} curve is related to a necessary condition for projectile instability. If the nutational frequency is less than the maximum of C_R, there are two times at which instability might develop. The C_{I1} and C_{R2} curves are rather typical, but the C_{I2} curve is not because it has a maximum at $t = 195$ and an inflection point at $t = 170$; these make it difficult to obtain a first guess for C_2. The problems encountered in calculating C_2 for $t \leq 200$

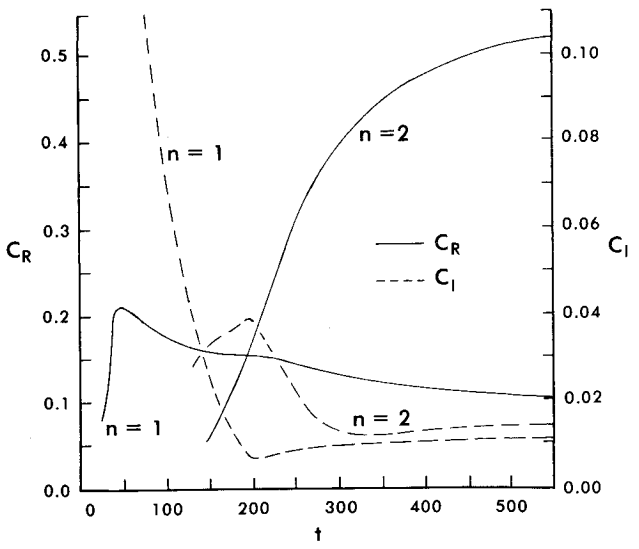

Fig. 4 Time histories for C_1 and C_2 for case 1, modes (3, 1, 1) and (3, 2, 1), $t_s = 460$, $\kappa = 0.5$.

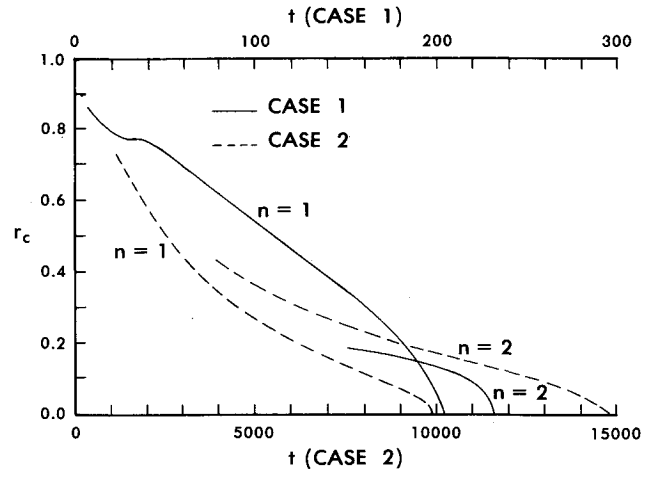

Fig. 5 Critical level r_c vs t for cases 1 and 2, $n = 1$ and 2, $\kappa = 0.5$.

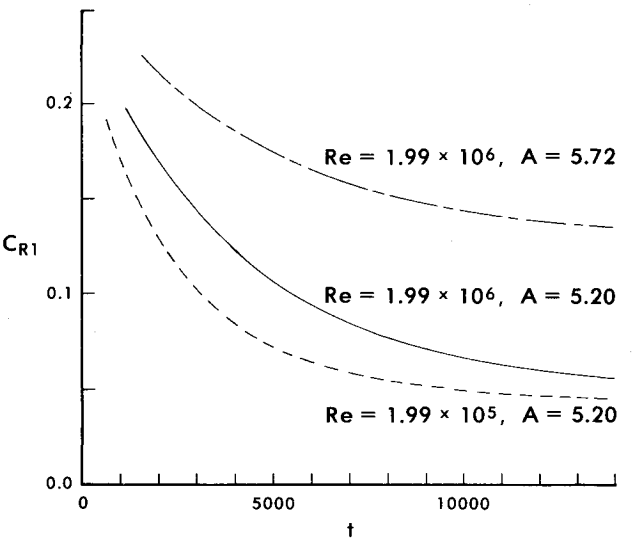

Fig. 6 C_{R1} vs t for case 2 and two variations.

Table 2 Effect of neglecting diffusion

	With diffusion			Without diffusion			
t	C_R	$C_I \times 10^3$	r_c	C_R	$C_I \times 10^3$	r_c	r_f
600	0.149	17.1	0.423	0.232	27.2	0.668	0.618
1245	0.0855	3.14	—	0.132	4.44	0.392	0.368

were discussed earlier. Since $C_{I2} < C_{I1}$ for $t < 140$, the $n = 2$ mode could be more significant than the $n = 1$ mode for projectile instability.

The variation of r_c with t is shown in Fig. 5 for both cases 1 and 2 and $n = 1$ and 2. Note the two time scales. For both cases $r_c = 0$ at earlier time for $n = 1$. The r_c for $n = 1$ and 2 are equal when $C_{R1} = C_{R2}$, but $C_{I1} \neq C_{I2}$ and the eigenfunctions are distinct. For case 1, $n = 1$, $r_c = 0$ at $t = 225 = 0.489 t_s$ and for case 2, $n = 1$, $r_c = 0$ at $t = 9950 = 3.76 t_{st}$ which gives $\bar{t} = 13.2$ s. Thus, for case 2 the critical layer exists over a substantial part of the projectile flight time; however, its effects are not great when r_c is small.

As a digression, consider the implications of using Eq. (3), which neglects diffusion terms, to determine the basic flow V profiles. Its solution is Eq. (6) for $r \geq r_f$ and zero otherwise. In Table 2, the e.v. and r_c determined this way are compared with those using the V including diffusion for $Re = 39{,}771$, $A = 3.12$, $t_s = 1245$, mode (3,1,1) and $\kappa = 0.5$. Neglecting diffusion gives large errors in C and r_c, and the r_c is never zero except in the limit $t \to \infty$.

The C_R time history for case 2, mode (5,1,1) using the turbulent Ekman layer compatibility condition [Eq. (5)] is given in Fig. 6; the maximum occurs for $t < 1200$. Results for two variations of parameters are also shown in Fig. 6: Re was decreased by a factor of 10 keeping A fixed, which decreased C_R; and A was increased by 10% keeping Re fixed, which increased C_R; the relative changes vary with t. In the first variation Re is in the transition range, but the turbulent Ekman layers were assumed. There is a large change in $r_c(t)$ for the first variation, e.g., $r_c = 0$ at $t = 3200$ compared to 9950 for case 2. For the second variation, $r_c(t)$ does not differ much from case 2, e.g., $r_c = 0$ at $t = 11{,}700$. The spin-up times are 1671 and 2912 for the first and second variations, respectively.

The rapid change in phase of the velocity across the critical layer in the O-S case is well known.[12] In the rotating fluid case, the change in phase of u' for $0 \leq r < 1$ will be shown. From Eq. (8)

$$u' = \left(u_R^2 + u_I^2\right)^{\frac{1}{2}} e^{-C_I t} \cos Kz' \sin\left[\beta - (C_R t - m\theta)\right]$$

$$\tan\beta = -u_R/u_I \tag{14}$$

The phase angle $\beta(r)$ is plotted in Fig. 7 for case 2. The rapid change in phase in the critical layer is evident for $t = 2000$, 6000, and 9000; the magnitude of the phase change in the critical layer is approximately 225, 175, and 180 deg, respectively. Another rapid change in β takes place in the sidewall boundary layer. This phase angle change is a sensitive indication of the critical layer. As t increases, the r interval over which β is essentially constant increases. For the conditions of Fig. 7, β = constant, except in the boundary layer, for $t \geq 10{,}000$ for which $r_c = 0$.

Discussion

The theory and a method for the solution of the spin-up e.v. problem were presented here. The theory for the perturbed flow is a linear one, but not for the basic flow. Because viscous effects are important in the sidewall boundary and critical layers, viscous perturbations are used. The theory has limitations because of the various assumptions that are made. The theory and method are successful in the sense that they provide results that are physically meaningful and do not

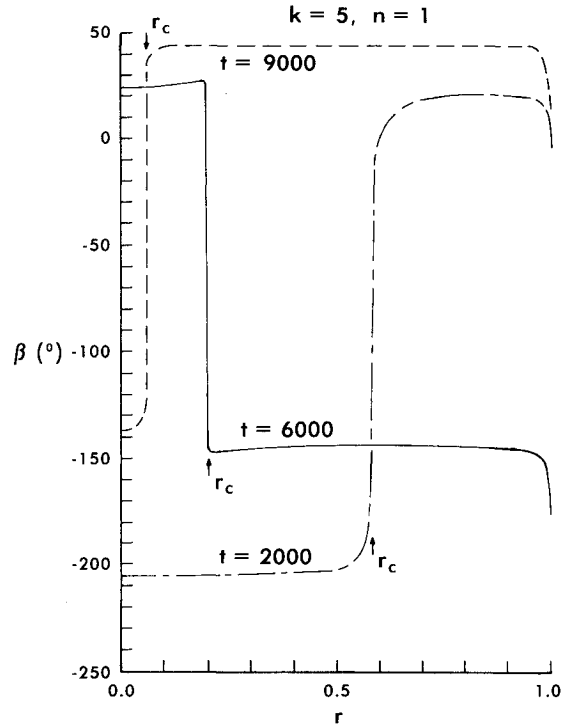

Fig. 7 Phase angle of u' for case 2 at three times.

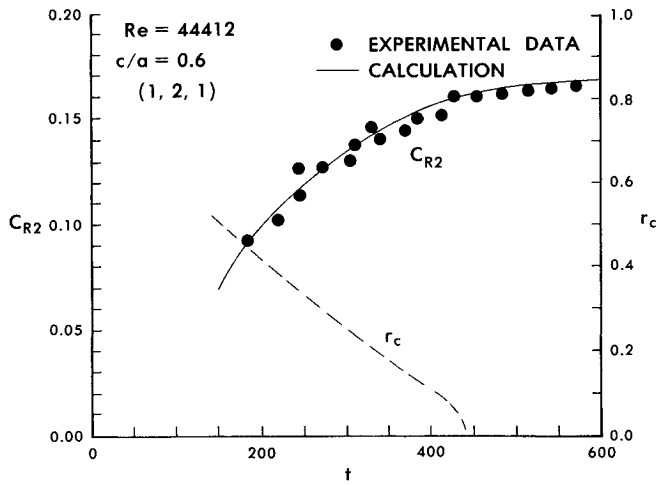

Fig. 8 C_R vs t: experimental points and calculated values; r_c vs t. $\kappa = 0.443$.

violate intuition or the "physics of the problem." Other investigators have worked on this problem without success in that sense. The more important gage of success is validation by comparison with either experimental results or numerical simulation.

For the solid rotation case and $m = 0$, a detailed validation was given in Ref. 3 using numerical simulation. This provides confidence in the treatment of Eq. (9) and the solid rotation endwall correction, for that case. Spin-up and $m = 0$ could be validated in the same way. It would require relatively more analysis to reduce the numerical data. At the present time, there is no numerical simulation to validate the $m = 1$ case. There are no data in the spin-up range from projectile firings that can be used to validate the theory.

To the authors' knowledge, the only reported measurements of C for $m = 1$ are in Refs. 6 and 13. Some experimental results for C_R vs t using the methods of Refs. 6 and 13 are shown in Fig. 8. For all points $4.39 \le Re \times 10^{-4} \le 4.45$, a negligible variation. The aspect ratio $A = 0.600$ and the mode is (1,2,1). The scatter in the data is about $\pm 3\%$ except at $t = 245$, where it is $\pm 5\%$. The calculated C_R, using $\kappa = 0.443$, is within the scatter of the data. This comparison validates the calculation of C_R for these parameters over the range of the data $0.724 \le t/t_s \le 2.252$. For large t, essentially at solid rotation, the experimental and calculated results differ by 1.5%.[6] The $r_c(t)$ curve shows that the critical layer exists over a considerable range for which data are presented.

The percentage differences of C_R, the frequency with respect to an inertial frame, are considerably larger than those for the frequency with respect to the rotating frame, C_{Rr}. For solid rotation, or steady state, it is more conventional to work in the rotating frame.[4] The relationships between the two frequencies and their percentage changes are

$$C_R = 1 - C_{Rr}$$

$$\Delta C_R / C_R = -(\Delta C_{Rr}/C_{Rr})(1 - C_R)/C_R$$

Comparisons of experimental and calculated C_R for modes (2,1,0) and (1,1,1) give the same conclusions as for the (1,2,1). Comparisons of C_I are not shown for two reasons: 1) the experimental error in the determination of C_I can be quite large; and 2) not accounting for the Ekman layers in the calculation gives C_I about one-half of the proper values; the effect on C_R is 1-2%.

References

[1]Wedemeyer, E.H., "The Unsteady Flow Within a Spinning Cylinder," *Journal of Fluid Mechanics*," Vol. 20, Pt. 3, 1964, pp. 383-399.

[2]Sedney, R. and Gerber, N., "Oscillations of a Liquid in a Rotating Cylinder: Part II. Spin-Up," ARBRL-TR-02489 (AD A129094), May 1983.

[3]Sedney, R., Gerber, N., and Bartos, J.M., "Oscillations of a Liquid in a Rotating Cylinder," AIAA Paper 82-0296, Jan. 1982; also ARBRL-TR-02488 (AD A129088), May 1983.

[4]Greenspan, H.P., *The Theory of Rotating Fluids*, Cambridge University Press, London and New York, 1968, Secs. 2.4 and 3.7.

[5]Benton, E.R. and Clark, A. Jr., "Spin-Up," *Annual Review of Fluid Mechanics*, Vol. 6, Annual Reviews, Inc., Palo Alto, Calif., 1974, p. 257-280.

[6]Stergiopoulos, S., "An Experimental Study of Inertial Waves in a Fluid Contained in a Rotating Cylindrical Cavity During Spin-Up from Rest," Ph.D. Thesis, York University, Toronto, Ontario, Feb. 1982.

[7]Sedney, R. and Gerber, N., "Viscous Effects in the Wedemeyer Model of Spin-Up from Rest," ARBRL-TR-02493 (AD A129506), June 1983.

[8]Sedney, R. and Gerber, N., "Treatment of the Discontinuity in the Spin-Up Problem with Impulsive Start," ARBRL-TR-02520 (AD A133682), Sept. 1983.

[9]Davey, A., "A Simple Numerical Method for Solving Orr-Sommerfeld Problems," *Quarterly Journal of Mathematics and Applied Mechanics*, Vol. 26, Pt. 4, 1973, pp. 401-411.

[10]Kitchens, C.W. Jr., Gerber, N., and Sedney, R., "Oscillations of a Liquid in a Rotating Cylinder: Part I. Solid-Body Rotation," ARBRL-TR-02081 (AD A057759), June 1978.

[11]Stewartson, K., "Marginally Stable Inviscid Flows with Critical Layers," *Journal of Applied Mathematics*, Vol. 27, 1981, pp. 133-175.

[12]Schlichting H., *Boundary Layer Theory*, 4th Ed., McGraw-Hill Book Co., New York, 1960, Chap. XVI.

[13]Aldridge, K. and Stergiopoulos, S., "Direct Measurement of Time-Dependent Complex Eigenfrequencies," submitted to *Experiments in Fluids*.